

Optical coherence tomography angiography of choroidal neovascularization in long-chain 3-hydroxyacyl-CoA dehydrogenase deficiency (LCHADD)



Nida Wongchaisuwat ^{a,b}, Jie Wang ^a, Paul Yang ^a, Lesley Everett ^{a,c}, Ashley Gregor ^c, Jose Alain Sahel ^d, Ken K. Nischal ^{d,e}, Mark E. Pennesi ^{a,c}, Melanie B. Gillingham ^c, Yali Jia ^{a,*}

^a Casey Eye Institute, Department of Ophthalmology, Oregon Health & Science University, Portland, OR, USA

^b Department of Ophthalmology, Faculty of Medicine Siriraj Hospital, Mahidol University, Bangkok, Thailand

^c Department of Molecular and Medical Genetics, Oregon Health and Science University, Portland, OR, USA

^d Vision Institute, University of Pittsburgh Medical Center and School of Medicine, Pennsylvania, USA

^e UPMC Children's Hospital, Pennsylvania, USA

ARTICLE INFO

Keywords:
Long-chain 3-hydroxyacyl-CoA dehydrogenase deficiency
LCHADD retinopathy
Choroidal neovascularization
CNV
OCT angiography

ABSTRACT

Purpose: To report the clinical utility of optical coherence tomography angiography (OCTA) for demonstrating choroidal neovascularization (CNV) associated with Long-Chain 3-Hydroxyacyl-CoA Dehydrogenase Deficiency (LCHADD) retinopathy.

Methods: Thirty-three participants with LCHADD (age 7–36 years; median 17) were imaged with OCTA and the Center for Ophthalmic Optics & Lasers Angiography Reading Toolkit (COOL-ART) software was implemented to process OCTA scans.

Results: Seven participants (21%; age 17–36 years; median 25) with LCHADD retinopathy demonstrated evidence of CNV by retinal examination or presence of CNV within outer retinal tissue on OCTA scans covering 3 × 3 and/or 6 × 6-mm. These sub-clinical CNVs are adjacent to hyperpigmented areas in the posterior pole. CNV presented at stage 2 or later of LCHADD retinopathy prior to the disappearance of RPE pigment in the macula.

Conclusion: OCTA can be applied as a non-invasive method to evaluate the retinal and choroidal microvasculature. OCTA can reveal CNV in LCHADD even when the clinical exam is inconclusive. These data suggest that the incidence of CNV is greater than expected and can occur even in the early stages of LCHADD retinopathy.

1. Introduction

Mitochondrial fatty acid beta-oxidation (FAO) is a major source of energy for many tissues in the human body, such as the heart, liver, and skeletal muscle. Previous dogma has suggested that retinal metabolism primarily relies on glucose oxidation for energy production, but newer studies suggest a role for mitochondrial FAO in retinal metabolism.^{1,2} Specific deficits in the multienzyme complex called the mitochondrial trifunctional protein (TFP) can cause pigmentary chorioretinopathy in infancy or childhood.³ TFP is composed of two alpha subunits that express the long-chain 2-enoyl-CoA hydratase and long-chain 3-hydroxyacyl-CoA dehydrogenase (LCHAD) activities while another two beta subunits mediate the beta-ketothiolase activity.⁴⁻⁸ These subunits are

encoded by Hydroxyacyl-CoA Dehydrogenase/3-Ketoacyl-CoA Thiolase/Enoyl-CoA Hydratase, Alpha subunit (*HADHA*) and Hydroxyacyl-CoA Dehydrogenase/3-Ketoacyl-CoA Thiolase/Enoyl-CoA Hydratase, Beta subunit (*HADHB*) genes. Autosomal recessively inherited pathogenic variants in both *HADHA* and *HADHB* have been described in humans. Several pathogenic variants in *HADHA* and *HADHB* impact TFP stability and expression and lead to a decrease in all three enzyme activities of TFP.⁹ However, the most common pathogenic variant is c.1528 G > C in the *HADHA* gene which leads to isolated LCHAD deficiency with relatively intact hydratase and ketothiolase activity. As a result, patients with the c.1528 G > C variant have elevated 3-hydroxy-fatty acids and 3-hydroxyacylcarnitines in plasma.¹⁰ The majority of other pathogenic variants in *HADHA* or *HADHB* cause

* Corresponding author. Casey Eye Institute, Department of Ophthalmology, Oregon Health & Science University, 515 SW Campus Rd, Mailcode CEI, Portland, OR 97239, USA.

E-mail address: jiaya@ohsu.edu (Y. Jia).

unstable protein expression and complete loss of protein function, resulting in TFP deficiency with lower plasma 3-hydroxy-fatty acids. However, accumulation of the various 3-hydroxy species seems more deleterious to retinal function than complete loss of TFP function.^{11,12}

The ocular manifestations in LCHAD deficiency first start as a progressive pigmentary change in the retina. Tyni et al. proposed four stages of LCHADD retinopathy starting from a normal fundus at birth, followed by stage 2, retinal pigment epithelium (RPE) pigment dispersion and clumping in the fovea. In stage 3, circumscribed central chorioretinal atrophy and pigmentary changes migrate toward the periphery. Finally, in stage 4, central scotomas developed from progressive loss of photoreceptors and almost complete diffuse chorioretinal atrophy.¹¹

Choroidal neovascularization (CNV) can be a serious cause of vision loss, although CNV is rare among children, it is one of the complications which can be observed in multiple inherited chorioretinal dystrophies (IRDs), such as vitelliform dystrophies, pattern dystrophy, gyrate atrophy or choroideremia.^{13,14} However, only one case report from Riccardo et al. has described the presence of CNV associated with a 21-year-old with LCHADD.¹⁵ The paucity of reported cases may be related to the reliance on fluorescein angiography (FA) to detect CNV. While FA is the gold standard to detect CNV in diseases such as age-related macular degeneration, detecting CNV in inherited retinal degenerations can be masked by chorioretinal atrophy, outer debris, or vitelliform material. Optical coherence tomography angiography (OCTA) provides a noninvasive imaging modality to study the morphology of neovascular membranes and retinochoroidal microvasculature.¹⁶ OCTA has the advantage of resolving vasculature at different retinal depths and is less impacted by windowing defects than FA. In this study, we report seven cases of CNV from OCTA images in subjects with LCHADD retinopathy. CNV appears to be a potential complication starting as early as stage 2 LCHADD retinopathy.

2. Materials and methods

Patients were enrolled after informed consent was obtained in accordance with a protocol approved by the Institutional Review Board of the University of Pittsburgh and adhering to the tenets of the Declaration of Helsinki. Here we describe seven patients who visited the ophthalmic genetics clinic at the Casey Eye Institute and University of Pittsburgh from January 2020 through December 2022 and were imaged with OCTA and demonstrated CNV.

These participants were enrolled in the Observational Natural History of LCHADD Retinopathy Study (R01 HD095968). The inclusion criteria for this natural history study were patients aged between 2 and 60 years with a confirmed diagnosis of LCHADD or trifunctional protein deficiency (TFPD). Diagnosis of LCHADD/TFPD was confirmed by obtaining medical record results of acylcarnitine profiles, fatty acid oxidation probe studies in cultured fibroblasts, and/or genetic testing. For this report, we included all cases of presumed CNV with sufficient quality OCTA images. Exclusion criteria for this analysis were the presence of severe media opacities, such as advanced cataracts, or the inability to obtain an OCTA image. CNV was identified using 2 methods: first, we consider the patient's history and retinal examination, looking for evidence of subretinal hemorrhage, fluid, or scar tissue along with a history of anti-VEGF treatment. Second, we examine the presence of CNV flow in the outer retinal layers using OCTA.

The patients underwent an eye examination, including measurement of best-corrected visual acuity, slit-lamp biomicroscopy, color fundus photography (FF450; Carl Zeiss Meditec, Dublin, CA), fundus auto-fluorescence (Optos 200Tx; Optos PLC, Marlborough, MA), spectral-domain OCT (Spectralis; Heidelberg Engineering, Germany) and OCT angiography described below.

Participants were scanned in a 3 × 3-mm and 6 × 6-mm area centered on foveal avascular zone (FAZ) using three commercial spectral-domain OCTA systems: (1) Avanti (Optovue/Visionix, Inc.,

Freemont, CA) with 840-nm central wavelength and 70-kHz axial scan rate, (2) Solix (Optovue/Visionix, Inc., Freemont, CA) with 840-nm central wavelength and 120-kHz axial scan rate, and (3) Angioplex (Carl Zeiss Meditec, Inc., Dublin, CA) with 840-nm central wavelength and 68-kHz axial scan rate. Both the Avanti and Solix OCTA systems utilized the commercial version of split-spectrum amplitude-decorrelation angiography (SSADA) algorithm to detect reflectance changes between two consecutive B-scans acquired at same location.^{17–19} In Angioplex system, optical microangiography (OMAG) algorithm was applied to detect the flow signals.^{20–22} Projection-resolved OCTA (PR-OCTA) algorithm was applied to suppress projection artifacts through the entire OCTA volume.²³

OCTA volumes were processed using our custom COOL-ART (Center for Ophthalmic Optics & Lasers-Angiography Reading Toolkit) image processing software. Retinal layer boundaries of the vitreous and the inner limiting membrane (ILM), outer plexiform layer (OPL), and Bruch's membrane (BM) on structural OCT volume were segmented automatically.²⁴ The segmentation errors that occurred in the area with severe degenerative changes were manually corrected.²⁴ PR-OCTA volumes were used to visualize CNV on both *en face* and cross-sectional angiograms.²⁵

Several maximum projection *en face* images were generated to display the pathological changes, including (1) OCT angiograms of the outer retina, comprising the slab between the outer boundary of OPL and BM; *en face* OCT angiograms of the inner retina, comprising the slab between the ILM and outer boundary of OPL. And (2) *en face* structural OCT of ellipsoid zone (EZ) slab.

3. Results

There were 40 patients enrolled in the Natural History of LCHADD retinopathy study, and OCT angiograms were obtained from 33 patients ranging in age from 7 to 36 years. Six patients were excluded because they were too young to obtain imaging, and one patient was excluded because of poor-quality photos. Nine eyes from seven patients diagnosed with LCHADD (age 17–36 years) complicated by CNV were included in this study. Genetic testing details for each case are presented in Table 1. All subjects were diagnosed of LCHADD, caused by pathogenic variants in HADHA gene (gene OMIM#600890) and all inherited in autosomal recessive pattern. FA was not performed in all cases due to the inactivity of the CNV disease. The prevalence of CNV in at least one eye in our study was 21 %. Patients with a CNV in at least one eye were older than those with no evidence of CNV ($p = 0.002$ Mann Whitney test).

3.1. Case 1

A 29-year-old man was diagnosed with LCHADD at birth from multiple organ involvement, including hypertrophic cardiomyopathy, liver dysfunction, myopathy, and myoglobinuria. His brother died from LCHADD complications at 9 months old. He harbored homozygous c.1528 G > C pathogenic variants in HADHA. His first fundus photographs were taken at age 6, at which time his visual acuity was 20/50 in his right eye and count finger in his left eye. A retinal exam revealed pigment accumulation in the central fovea of both eyes, and a small area of fibrotic membrane was observed just temporal to foveal pigmentation in his right eye (Fig. 1A). After multiple follow-up visits, macular pigment disappeared and progressed into choroidal atrophy in the left eye, while the right eye demonstrated a white fibrotic scar with adjacent dense well-demarcated pigment clumping in the foveal area (Fig. 1B). At age 29, his LCHADD retinopathy was Stage 3, but his vision remained stable at 20/50, and there was no recorded evidence of subretinal hemorrhage or fluid. OCTA was performed at age 28 and revealed a CNV plexus lying in the outer retinal space underneath the foveal pigmentation. Images from the choriocapillaris slab revealed a more extensive fibrovascular network extending from the peripapillary area to the temporal fovea (Fig. 1C–E).

Table 1
Subject disease variants and testing.

Subject	Variants	Lab	Technique	CLIA (Y/N)
1	Homozygous c.1528G > C (Pathogenic) (1)	Dr. Arnold Strauss Prevention Genetics	Sanger Sanger	N Y
2	c.1528G > C (Pathogenic)/ c.479_482delinsATA (Novel, Likely pathogenic)		NGS +	
3	Homozygous c.1528G > C (Pathogenic)	NA	NA	NA
4	Homozygous c.1528G > C (Pathogenic)	Dr. Arnold Strauss	Sanger	N
5	c.1528G > C (Pathogenic)/ c.1620 + 2_1620+6delTAAGG (IVS15 + 2_+6delTAAGG) (Pathogenic) (2)	Emory Genetics Lab	Targeted Testing	Y
6	Homozygous c.1528G > C (Pathogenic)	Dr. Kerr Barnes Jewish Hospital	PCR-RFLP	N
7	Homozygous c.1528G > C (Pathogenic)	Dr. Arnold Strauss, Yale	Sanger	N

Abbreviations: NGS = Next Generation Sequencing; CLIA = Clinical Laboratory Improvement Amendments; PCR-RFLP = Polymerase Chain Reaction-Restriction Fragment Length Polymorphism; NA = data was not available in the medical record.

1. Sims HF, Brackett JC, Powell CK, Treem WR, Hale DE, Bennett MJ, Gibson B, Shapiro S, Strauss AW. The molecular basis of pediatric long chain 3-hydroxyacyl-CoA dehydrogenase deficiency associated with maternal acute fatty liver of pregnancy. Proceedings of the National Academy of Sciences of the United States of America. 1995; 92(3):841–845. Structured.

2. Ibdah, J. A., Bennett, M. J., Rinaldo, P., Zhao, Y., Gibson, B., Sims, H. F., & Strauss, A. W. A fetal fatty-acid oxidation disorder as a cause of liver disease in pregnant women. *N Engl J Med*, 1999; 340(22), 1723–1731. doi:10.1056/nejm199906033402204.

3.2. Case 2

A 32-year-old woman who had two different variants identified in *HADHA*; the c.1528 G > C common pathogenic variant and c.479_482delinsATA a potential pathogenic variant and was delivered at the gestational age of 30 weeks due to maternal acute fatty liver. She had episodes of hypoglycemia, liver and kidney failure, myoglobinuria, peripheral neuropathy, rhabdomyolysis, and cardiomegaly. Her visual symptom started with nyctalopia at age 14. At that time, her visual acuity was counting fingers in her right eye and 20/30 in her left eye. Fundus photos demonstrated central pigment clumping in the right fovea, generalized retinal pigment epithelium (RPE) granularity, and mottling with partial choroidal atrophy in the posterior pole of both eyes, consistent with stages 2–3 of LCHADD retinopathy. Over the next 18 years, there was a progressive increase in foveal pigmentation and the development of choroidal atrophy starting centrally perifoveal and spreading outwards to result in Stage 4 LCHADD retinopathy (Fig. 2). OCTA images from the right eye at age 31 demonstrated a neovascular plexus in the outer retinal slab (between the outer boundary of OPL and BM) adjacent to the central fovea. This finding suggests a diagnosis of subclinical CNV from OCTA (Fig. 2C).

3.3. Case 3

A 26-year-old woman was diagnosed with LCHADD at 8 months old upon presenting with a hypoglycemic crisis. Her genotype was homozygous for the common pathogenic variant c.1528 G > C. She also had a history of cardiomyopathy, hepatopathy, rhabdomyolysis, and mood disorder. At age 10, while her vision was stable at 20/20 in both eyes, she developed bilateral macular pigment clumping and scattered bone spicules in the peripheral retina. She complained of worsening vision in both eyes at age 16 following an acute metabolic decompensation and

hospitalization for rhabdomyolysis. Her visual acuity dropped to 20/25 in the right eye and 20/100 in the left eye. Retinal examination at that time revealed a subretinal green-tinged membrane nasal to fovea without hemorrhage or fluid in the left eye. Without any treatment, the green-tinged membrane evolved into a subretinal white scar over time, and vision stabilized. Similar to the previous cases, the pigmentary atrophy in the right eye spread from the central macula to outside the vascular arcades. The left eye had persistent macular pigment clumping adjacent to the fibrotic scar with slight enlargement of the scar over time, resulting in a stage 3 retinopathy. OCTA images of the left eye (Fig. 3) were taken at age 25. They demonstrated a neovascular lesion in the subretinal space underneath the pigmentation and was composed predominantly of large diameter vessels originating from the peripapillary area. There was no CNV in the right eye.

3.4. Case 4

An 18-year-old man homozygous for c.1528 G > C pathogenic variant was diagnosed with LCHADD by newborn screening. He had a history of multiple episodes of rhabdomyolysis and myoglobinuria. His retinopathy started at age 3 when diffuse pigmentary speckling in the peripheral retina was observed, but visual acuity measured 20/20 in his right eye and 20/40 in his left eye. By age 6, there was an increase in foveal pigmentation in both eyes with asymptomatic subretinal hemorrhage at the superonasal edge of the RPE clumping in the left eye. OCT during that same visit revealed elevated and clumped RPE, cystoid macular edema (CME), and loss of photoreceptor in the left eye. He was diagnosed with CNV and received intravitreal injections of bevacizumab 1.25 mg in the left eye. After treatment, the best corrected visual acuity improved from 20/70 to 20/40 OS with a resolution of the subretinal hemorrhage. The second dose of bevacizumab was given 5 months later, and the CNV regressed into a subfoveal fibrovascular lesion with RPE atrophy and focal hyperpigmented clumping. No further treatment was given. At age 10, his right eye developed a subretinal fibrotic scar with a pigment epithelial detachment (PED) seen by OCT, and the lesion was stable for 8 years. OCTA was obtained at age 18. Unfortunately, signal quality from the left eye was poor. However, in the right eye, a plexus of dense capillary networks were observed underneath the RPE located superior to the foveal pigmentation, suggesting type 1 CNV (Fig. 4).

3.5. Case 5

A 17-year-old woman was diagnosed with LCHADD at 5 months old upon presenting with hypoglycemia, liver dysfunction, and cardiomyopathy. She had two different variants in *HADHA*; the c.1528 G > C common pathogenic variant and c.1620 + 2_1620+6delTAAGG likely pathogenic variant. Her best corrected visual acuity was 20/125 in her right eye and 20/400 in her left eye. Retinal examination revealed diffuse pigmentary change and atrophic choroid in the central macula. OCTA depicted bilateral CNV membranes (Fig. 5A and B).

3.6. Case 6

A 36-year-old woman had been diagnosed with LCHADD from a history of siblings with LCHADD and had a hypoglycemic episode at birth. She was homozygous for c.1528 G > C pathogenic variant. She also had a history of rhabdomyolysis, neuropathy, and retinopathy. Her fundus examination showed peripheral pigmentary clumping and central choroidal atrophy in both eyes. She did not report changes in her vision, and her visual acuity measured 20/40 in both eyes. OCTA was obtained at age 36, and a possible small area of CNV in the left eye was detected (Fig. 5C).

3.7. Case 7

Case 7 was a 21-year-old man who was homozygous for c.1528 G > C

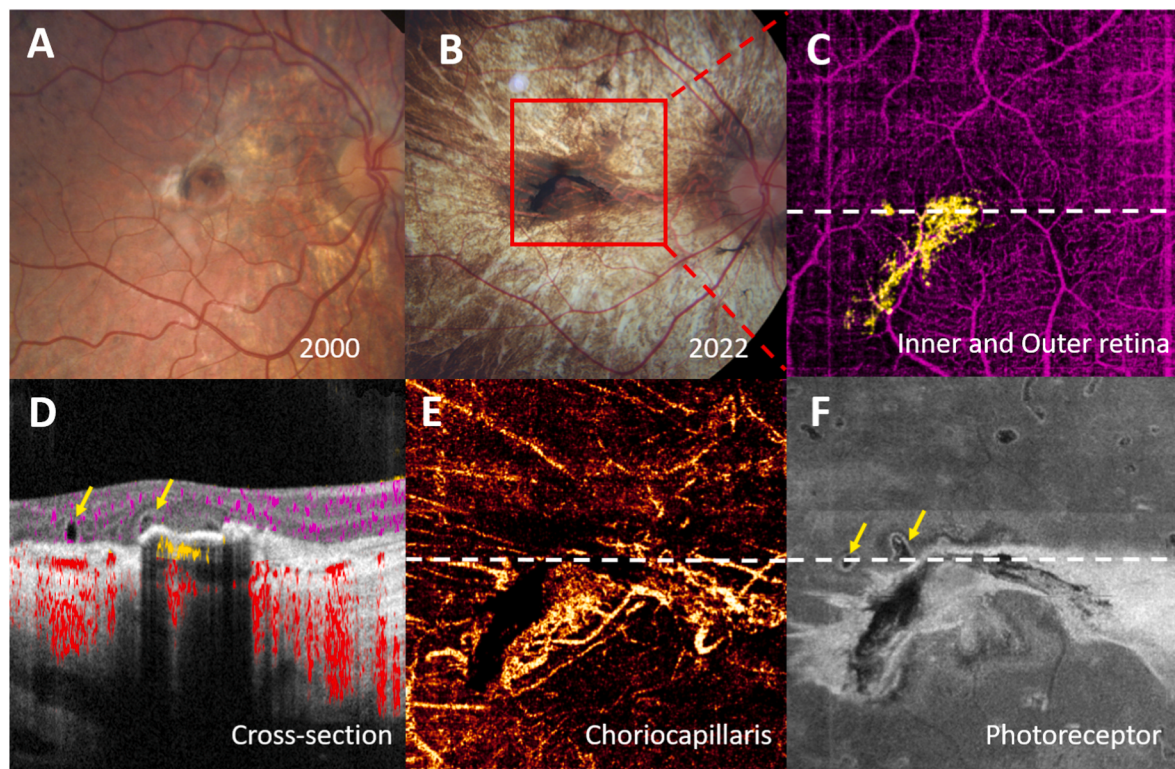


Fig. 1. Patient 1 of LCHADD complicated with CNV in the right eye. A, Color fundus photograph revealing a nummular hyperpigmented lesion in the right macula with a scar temporal and superonasal to the pigmented lesion. B, Color fundus photograph of the same patient after 22 years follow up showing extension of the dense hyperpigmented lesion and faint scar surrounded by a pale macular choroidal atrophy. C, After applying the projection resolved algorithm to a 6×6 mm red box area in B, color-coded composite *en face* OCTA, subretinal choroidal neovascular plexus (yellow) was highlighted D, Cross-sectional Spectral Domain-OCTA image corresponding to the white dot line in C showing subfoveal choroidal neovascularization E, *En-face* slab of choriocapillaris showing an enlarged area of subfoveal CNV network. F, *En-face* OCT slab of the photoreceptor demonstrated subretinal fibrotic scar. Retinal tubulation adjacent to the CNV were observed. (yellow arrow). (For interpretation of the references to color in this figure legend, the reader is referred to the Web version of this article.)

common pathogenic variant. He was born prematurely at 34 weeks due to maternal Hemolysis, Elevated Liver enzymes, and Low Platelets (HELLP) syndrome. He was diagnosed with LCHADD at 6 months of age following metabolic decompensation after a flu virus. He also had a history of hypoglycemic episodes, cardiomyopathy, rhabdomyolysis, and neuropathy. His retinopathy was first detected at age 5 when diffuse pigmentary speckling in the retina was observed. He began to have choroidal atrophy in the center of both eyes with a subretinal whitish lesion seen in the nasal area of the macula on the left eye from a fundus photo at age 7 while decreased visual acuity measured from 20/80 to 20/150 in his right eye and 20/25 to 20/125 in his left eye. Twelve years later, his visual acuity remains stable, 20/200 in his right eye and 20/100 in his left eye, his fundus had progressive chorioretinal atrophy of the posterior pole with a subretinal white scar persisting in the left eye resulting in Stage 4 retinopathy. OCTA was obtained at age 21, however, in the scans of the left eye, expected CNV flow was not detected, despite the white scar was presumed to have been a CNV.

Among the seven cases, five were common homozygous for c.1528 G > C HADHA variant. Genetic testing identified participant 2 was heterozygous for c.1528G > C and a variant designated c 479_482deffnsAA TA, which is predicted to result in a premature protein termination (p. lle160_Ale161dellnsLys*). To our knowledge, this variant has not been reported but is expected to be pathogenic. Participants 5 was heterozygous for c.1528 G > C and c.1620 + 2_1620+6delTAAGG, this variant has been reported previously and classified as pathogenic.²⁶ Mean visual acuity in the eyes of the CNV group was 44.8 ETDRS letters compared to 80.2 in non-CNV eyes ($p = 0.003$). If only advanced stages (3 and 4) were compared, mean visual acuity was significantly different between CNV and non-CNV eyes, with ETDRS letter score of 42 and 64.53, respectively ($p = 0.03$).

4. Discussion

CNV secondary to LCHADD retinopathy was previously thought to be a rare complication, however, it appears to occur more frequently and at earlier stages of progression than expected. The etiology of CNV in subjects with LCHADD retinopathy is still unknown. A recent study from Riccardo et al. demonstrated one case of LCHADD complicated by CNV. The pathophysiology is thought to begin from the atrophy of the choriocapillaris and medium-sized choroidal vessels, which leads to hypoxia in the posterior pole.¹⁵ Structural OCT revealed atrophic thinning of ONL, EZ, RPE, choriocapillaris, and choroidal layers in correspondence to the area of central macular atrophy and CNV. Our study observed the prevalence of CNV in 7 out of 34 cases (21%). The incidence of CNV associated with LCHADD might be higher. Still, it remains underdiagnosed in the clinical setting due to the quiescence of the disease and the lack of availability of OCTA in the past.

Our case series of seven patients demonstrate that the onset of CNV started at age six or earlier in three cases, age 16 in one case, and was subclinical in three cases, with CNV not being observed until OCTAs were obtained at ages 17, 29, and 36. Six patients did not complain of a change in vision at the time CNV occurred, while one presented with worsening vision.

Patients with LCHADD have episodic metabolic decompensation during periods of illness, fasting, or excessive exercise that leads to elevated long-chain 3-hydroxy fatty acids and carnitine esters in the plasma.²⁷ These partially oxidized fatty acids are observed even in healthy individuals with LCHADD; they rise after fasting and fall with eating.¹⁰ We have noted a correlation between chronic elevations of long-chain 3-hydroxyacylcarnitines and more rapid chorioretinopathy progression.^{12,28} Others have noted a correlation between increased

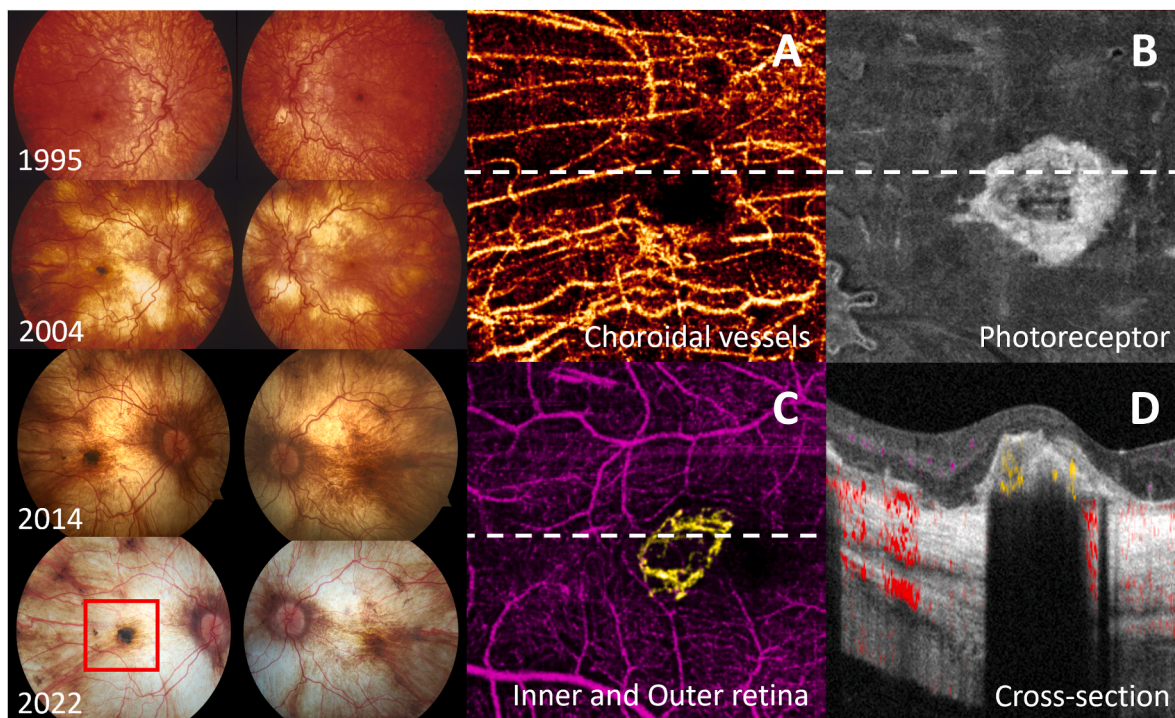


Fig. 2. Left column demonstrates a progression of the fundus changes in LCHADD in patient 2, starting at 6 years of age until 31 years of age. The retinal vessels are tortuous. RPE pigmentation is presented in the central fovea of both eyes. A peripapillary area of bare sclera has appeared and enlarged over time along with diminished pigment clumps in the central fovea in the left eye (non-affected eye). Finally, the bare sclera is visible over the whole posterior pole. Only a few large choroidal vessel trunks are seen in the center of the macula and temporal to it. Pigment clumping is persisted in the central macula of the right eye (affected eye). Red box delineates 6×6 mm area corresponding to OCTA images. The middle and right columns demonstrate OCTA images of CNV-associated LCHADD. A,B, *En face* OCTA slab at the choroidal layer and Ellipsoid zone of photoreceptor, showing the appearance of subfoveal choroidal neovascularization. C, Color composite *en face* OCTA of inner retinal vasculature (purple) and CNV vessels (yellow) in a circular pattern. D, Cross-sectional Spectral Domain-OCTA image corresponding to the white dot line in C showing type 2 neovascular membrane and pigment with relative flow (yellow) within the lesion. (For interpretation of the references to color in this figure legend, the reader is referred to the Web version of this article.)

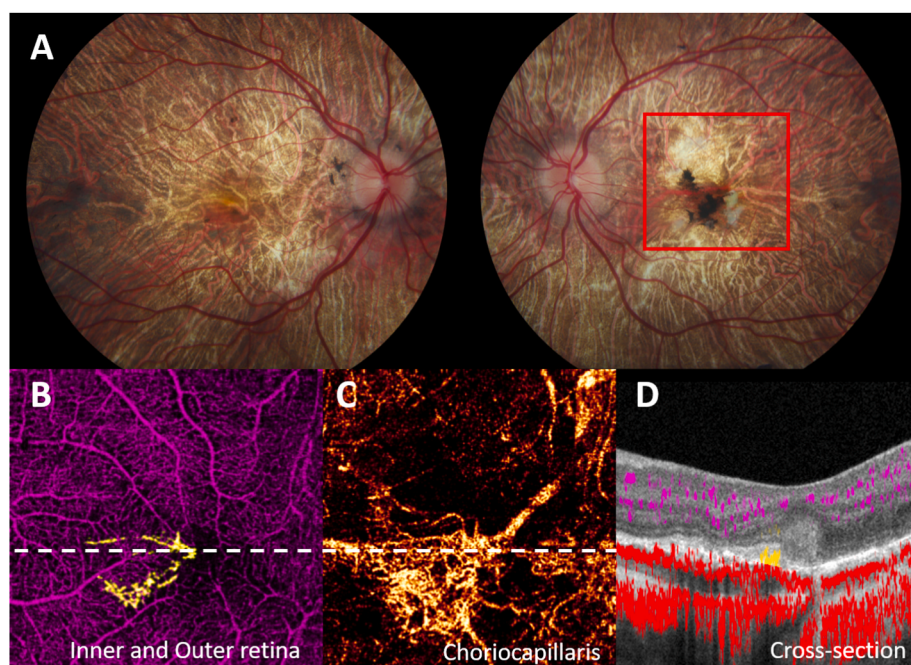


Fig. 3. Patient 3 of LCHADD complicated by CNV OS. A, Fundus photo shows diffuse chorioretinal atrophy OU with white fibrotic scar and pigment clumping at macula OS. Red box delineates a 6×6 mm area corresponding to OCTA images. B, 6×6 mm OCTA in inner and outer retinal slab revealed the CNV plexus (yellow). C, *En-face* slab of choriocapillaris showing an enlarged area of CNV network. D, segmented cross-sectional scan of OCTA of white dot line in B demonstrates angiographic flow (yellow) within subretinal hyperreflective tissue of left eye. (For interpretation of the references to color in this figure legend, the reader is referred to the Web version of this article.)

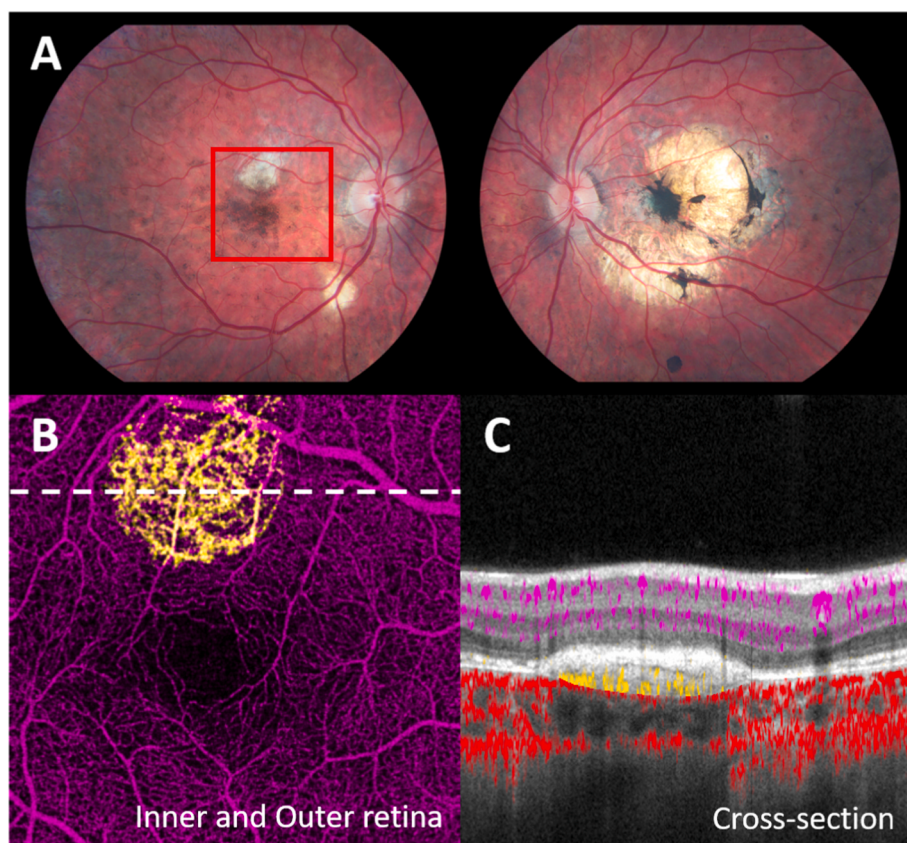


Fig. 4. Patient 4 of CNV associated LCHADD. A, Fundus photo shows subretinal white scar at perimacular region in stage 2 LCHADD retinoopathy OD, central choroidal atrophy and pigment clumping at macula OS from previous CNV. Red box delineates 6×6 mm area corresponding to B and C images. B, En-face 6×6 mm OCTA in outer retinal slab revealed the CNV plexus (yellow). C, Cross-sectional Spectral Domain-OCTA image at the white dot line in B showing type 1 neovascular membrane. (For interpretation of the references to color in this figure legend, the reader is referred to the Web version of this article.)

hospitalizations from metabolic decompensation and more rapid vision loss.^{29,30} However, no correlation between CNV and 3-hydroxyacylcarnitines has been previously reported. Rapid deterioration of visual function may have a role in initiating neovascularization in choroidal vessels.

For most cases, the CNV was detected during stage 2 of the retinopathy, corresponding to when pigment clumping in the fovea first appears, but visual acuity often remains intact. When the disease progresses to a later stage, the central pigmentation typically disappears, leading to macular chorioretinal atrophy with progression peripherally.³¹ Interestingly, we observed that in cases with CNV, the pigmentary clumping adjacent to the fibrovascular scar was intense and persisted over time. Melanosomes in RPE contain melanin-imbibing antioxidant properties such as sequestration of redox-active metal ions, and scavenging of free radicals, that help to protect the neural retina.^{32,33} We hypothesize that the remaining RPE melanosomes in CNV complicated LCHADD might be a protective mechanism. Another hypothesis for the hyperpigmented lesion is based on the pathogenesis of the Foster-Fuchs spot in myopic CNV. Similar to CNV in retinal dystrophy, most cases of myopic CNV are usually small and tend to regress spontaneously. These CNVs are associated with subretinal or choroidal hemorrhage, which is engulfed by proliferating retinal pigment epithelial cells. Therefore, the Fuchs spot usually presents with a central elevated hyperpigmented spot, surrounded by enlarged chorioretinal atrophy in the macula region.^{34,35}

Six out of seven patients demonstrated type 2 neovascularization which arises in the outer retinal space. In contrast, case 4 patient developed bilateral CNV with a type 1 membrane in the right eye and a type 2 membrane in the left eye. All were observed in a quiescent state and had evolved into fibrovascular membranes. Similar to other CNV

secondary to distinct retinal dystrophies,¹³ they tend to be small, focal, and inactive in nature. They can spontaneously subside or require only a few injections of anti-VEGF treatment to preserve vision. Although the CNV in LCHADD is subtle and rarely requires treatment, it might cause some degree of damage to photoreceptors causing deterioration of visual acuity. Our study observed a lower ETDRS letter score in eyes with CNV compared to eyes without CNV, although the sample size is small. Lower vision may be related to either photoreceptors disruption or tissue scarring at the CNV. However, this suggests the importance of early detection and close observation.

In the late course of the disease, choroidal atrophy and thinning progressed, resulting in the whitening of the macular area. This causes the indistinctness of the fibrotic scar when observed in color fundus photographs, and CNV can be missed. OCTA is a useful and non-invasive method to evaluate the CNV in this situation. We can segment retinal, RPE, and choriocapillaris layers on OCT/OCTA scans, which helps monitor the area of CNV and the progression of the disease over time. With the capability of OCTA, patients with CNV-associated LCHADD could be diagnosed at the early stage. They may have better visual outcomes if the treatment is given with intravitreal anti-VEGF before the CNV membrane converts to a fibrotic scar.

Our study has also demonstrated that device-agnostic software, such as the projection-resolved algorithm²⁵ in COOL-ART can be used for removing projection artifacts and retaining flow signals from CNV vessels while suppressing projected flow artifacts from retinal superficial and deep plexuses. As a result, the software can reliably detect volumetric flow in the CNV and can also be used to detect CNV lesions even when imaged from different devices.

Some limitations of our study were that CNV was detected retrospectively, and OCT angiograms were only available at the stages of CNV

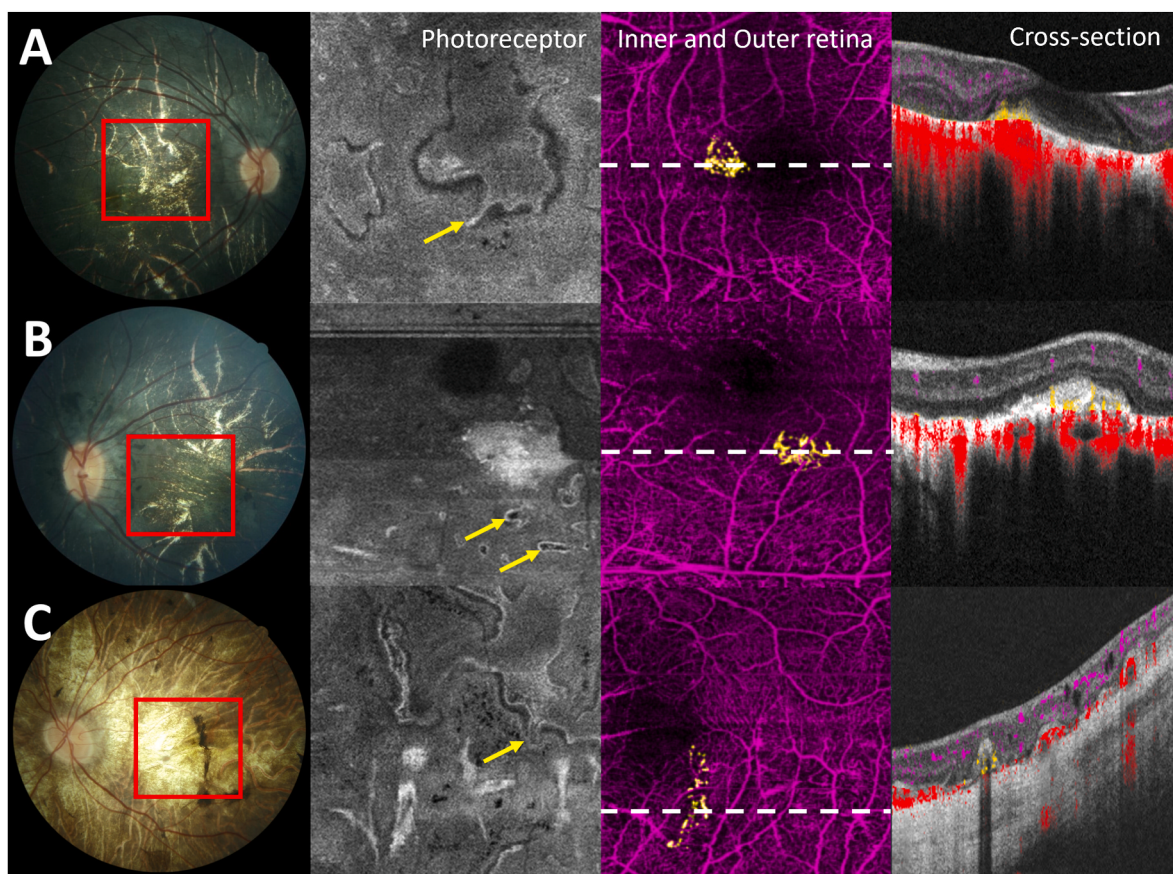


Fig. 5. A and B, patient 5 OD and OS respectively,C, patient 6 of CNV-associated LCHADD. First column is the fundus photographs of these two patients in advance stage, choroidal atrophy were observed in all cases with pigment clumping at macula OS in patient 6. Second column demonstrated *En face* OCTA slab of photoreceptors. Retinal tubulation were observed in difference patterns. (yellow arrow) Third column, *en-face* 6 × 6 mm OCTA in the outer retinal slab corresponding to area within the red boxes in column A revealed subretinal CNV plexus (yellow). The last column showed cross-sectional Spectral Domain-OCTA with color-coded flow overlay corresponding to white dot line in the third column, illustrated the angiographic flow of CNV (yellow). OCTA image of a bottom row from patient 6 revealed slightly low flow signal which possible a small CNV. (For interpretation of the references to color in this figure legend, the reader is referred to the Web version of this article.)

presentation. While 7 cases from 40 patients may appear to be a small sample size, the study is the largest reported cohort of patients with LCHADD/TFPD to date. Further studies are required to confirm the distinct nature of CNV in LCHADD compared to other forms of CNV. Newer technologies, such as OCT oximetry³⁶ to evaluate oxygen concentration in retinal and choroidal vasculature could potentiate a better understanding of the pathogenesis of the disease.

In conclusion, as a non-invasive method, OCTA was used to evaluate the retinal and choroidal microvasculature, including the presence of CNV in LCHADD. CNV is suspected to be greater than previously expected and occurs at an early stage of LCHADD retinopathy.

Financial disclosures

Jie Wang: Optovue/Visionix, Inc (P, R); Genentech, Inc. (P, R); Yali Jia: Optovue/Visionix, Inc. (P, R); Genentech, Inc. (P, F, R); Optos (P). These potential conflicts of interest have been reviewed and managed by OHSU. Other authors declare no conflicts of interest related to this article.

Declaration of competing interest

The authors declare the following financial interests/personal relationships which may be considered as potential competing interests: Jie Wang: Optovue/Visionix, Inc (P, R); Yali Jia: Optovue/Visionix, Inc. (P, R), Optos (P). These potential conflicts of interest have been

reviewed and managed by OHSU. Other authors declare no conflicts of interest related to this article.

Acknowledgments

This work was supported by the National Institute of Health (R01 HD095968, R01 EY027833, R01 EY035410, R01 EY024544, R01 EY031394, R01 EY023285, T32 EY023211, UL1TR002369, P30 EY010572); the Malcolm M. Marquis, MD Endowed Fund for Innovation; an Unrestricted Departmental Funding Grant and Dr. H. James and Carole Free Catalyst Award from Research to Prevent Blindness (New York, NY), Edward N. & Della L. Thome Memorial Foundation Award, and the Bright Focus Foundation (G2020168, M20230081).

References

- Tyni T, Paetau A, Strauss AW, Middleton B, Kivelä T. Mitochondrial fatty acid beta-oxidation in the human eye and brain: implications for the retinopathy of long-chain 3-hydroxyacyl-CoA dehydrogenase deficiency. *Pediatr Res.* 2004;56(5):744–750.
- Harding CO, Gillingham MB, van Calcar SC, Wolff JA, Verhoeve JN, Mills MD. Docosahexaenoic acid and retinal function in children with long-chain 3-hydroxyacyl-CoA dehydrogenase deficiency. *J Inherit Metab Dis.* 1999;22(3):276–280.
- Tyni T, Johnson M, Eaton S, Pourfarzam M, Andrews R, Turnbull DM. Mitochondrial fatty acid β-oxidation in the retinal pigment epithelium. *Pediatr Res.* 2002;52(4):595–600.
- Xia C, Fu Z, Battaile KP, Kim JP. Crystal structure of human mitochondrial trifunctional protein, a fatty acid β-oxidation metabolon. *Proc Natl Acad Sci U S A.* 2019;116(13):6069–6074.

5. Liang K, Li N, Wang X, et al. Cryo-EM structure of human mitochondrial trifunctional protein. *Proc Natl Acad Sci U S A*. 2018;115(27):7039–7044.
6. Fletcher AL, Pennesi ME, Harding CO, Weleber RG, Gillingham MB. Observations regarding retinopathy in mitochondrial trifunctional protein deficiencies. *Mol Genet Metabol*. 2012;106(1):18–24.
7. Rinaldo P, Matern D, Bennett MJ. Fatty acid oxidation disorders. *Annu Rev Physiol*. 2002;64:477–502.
8. Spiekerkoetter U. Mitochondrial fatty acid oxidation disorders: clinical presentation of long-chain fatty acid oxidation defects before and after newborn screening. *J Inher Metab Dis*. 2010;33(5):527–532.
9. Boutron A, Acquaviva C, Vianey-Saban C, et al. Comprehensive cDNA study and quantitative analysis of mutant HADHA and HADHB transcripts in a French cohort of 52 patients with mitochondrial trifunctional protein deficiency. *Mol Genet Metabol*. 2011;103(4):341–348.
10. Elizondo G, Matern D, Vockley J, Harding CO, Gillingham MB. Effects of fasting, feeding and exercise on plasma acylcarnitines among subjects with CPT2D, VLCADD and LCHADD/TFPD. *Mol Genet Metabol*. 2020;131(1–2):90–97.
11. Tyni T, Kivelä T, Lappi M, Summanen P, Nikoskelainen E, Pihko H. Ophthalmologic findings in long-chain 3-hydroxyacyl-CoA dehydrogenase deficiency caused by the G1528C mutation: a new type of hereditary metabolic chorioretinopathy. *Ophthalmology*. 1998;105(5):810–824.
12. Boese EA, Jain N, Jia Y, et al. Characterization of chorioretinopathy associated with mitochondrial trifunctional protein disorders: long-term follow-up of 21 cases. *Ophthalmology*. 2016;123(10):2183–2195.
13. Marano F, Deutman AF, Leys A, Andekerke AL. Hereditary retinal dystrophies and choroidal neovascularization. *Graefes Arch Clin Exp Ophthalmol*. 2000;238(9):760–764.
14. Patel RC, Gao SS, Zhang M, et al. Optical coherence tomography angiography of choroidal neovascularization in four inherited retinal dystrophies. *Retina*. 2016;36(12):2339–2347.
15. Sacconi R, Bandello F, Querques G. Choroidal neovascularization associated with long-chain 3-hydroxyacyl-CoA dehydrogenase deficiency. *Retin Cases Brief Rep*. 2022;16(1).
16. Jia Y, Bailey ST, Wilson DJ, et al. Quantitative optical coherence tomography angiography of choroidal neovascularization in age-related macular degeneration. *Ophthalmology*. 2014;121(7):1435–1444.
17. Huang D, Jia Y, Gao SS, Lumbruso B, Rispoli M. Optical coherence tomography angiography using the Optovue device. *Dev Ophthalmol*. 2016;56:6–12.
18. Jia Y, Tan O, Tokayer J, et al. Split-spectrum amplitude-decorrelation angiography with optical coherence tomography. *Opt Express*. 2012;20(4):4710–4725.
19. Tokayer J, Jia Y, Dhalla AH, Huang D. Blood flow velocity quantification using split-spectrum amplitude-decorrelation angiography with optical coherence tomography. *Biomed Opt Express*. 2013;4(10):1909–1924.
20. Wang RK, An L, Francis P, Wilson DJ. Depth-resolved imaging of capillary networks in retina and choroid using ultrahigh sensitive optical microangiography. *Opt Lett*. 2010;35(9):1467–1469.
21. An L, Shen TT, Wang RK. Using ultrahigh sensitive optical microangiography to achieve comprehensive depth resolved microvasculature mapping for human retina. *J Biomed Opt*. 2011;16(10), 106013.
22. Zhang Q, Zhang A, Lee CS, et al. Projection artifact removal improves visualization and quantitation of macular neovascularization imaged by optical coherence tomography angiography. *Ophthalmol Retina*. 2017;1(2):124–136.
23. Wang J, Hormel TT, Bailey ST, Hwang TS, Huang D, Jia Y. Signal attenuation-compensated projection-resolved OCT angiography. *Biomed Opt Express*. 2023;14(5):2040–2054.
24. Zhang M, Wang J, Pechauer AD, et al. Advanced image processing for optical coherence tomographic angiography of macular diseases. *Biomed Opt Express*. 2015;6(12):4661–4675.
25. Wang J, Zhang M, Hwang TS, et al. Reflectance-based projection-resolved optical coherence tomography angiography [Invited]. *Biomed Opt Express*. 2017;8(3):1536–1548.
26. Ibdah JA, Bennett MJ, Rinaldo P, et al. A fetal fatty-acid oxidation disorder as a cause of liver disease in pregnant women. *N Engl J Med*. 1999;340(22):1723–1731.
27. Vockley J, Bennett MJ, Gillingham MB. Mitochondrial fatty acid oxidation disorders. In: Valle DL, Antonarakis S, Ballabio A, Beaudet AL, Mitchell GA, eds. *The Online Metabolic and Molecular Bases of Inherited Disease*. New York, NY: McGraw-Hill Education; 2019.
28. Gillingham MB, Weleber RG, Neuringer M, et al. Effect of optimal dietary therapy upon visual function in children with long-chain 3-hydroxyacyl CoA dehydrogenase and trifunctional protein deficiency. *Mol Genet Metabol*. 2005;86(1–2):124–133.
29. Fahnehjelm KT, Holmström G, Ying L, et al. Ocular characteristics in 10 children with long-chain 3-hydroxyacyl-CoA dehydrogenase deficiency: a cross-sectional study with long-term follow-up. *Acta Ophthalmol*. 2008;86(3):329–337.
30. Fahnehjelm KT, Liu Y, Olsson D, et al. Most patients with long-chain 3-hydroxyacyl-CoA dehydrogenase deficiency develop pathological or subnormal retinal function. *Acta Paediatr*. 2016;105(12):1451–1460.
31. Polinati PP, Ilmarinen T, Trokovic R, et al. Patient-specific induced pluripotent stem cell-derived RPE cells: understanding the pathogenesis of retinopathy in long-chain 3-hydroxyacyl-CoA dehydrogenase deficiency. *Invest Ophthalmol Vis Sci*. 2015;56(5):3371–3382.
32. Różanowski B, Burke JM, Boulton ME, Sarna T, Różanowska M. Human RPE melanosomes protect from photosensitized and iron-mediated oxidation but become pro-oxidant in the presence of iron upon photodegradation. *Invest Ophthalmol Vis Sci*. 2008;49(7):2838–2847.
33. Strauss O. The retinal pigment epithelium in visual function. *Physiol Rev*. 2005;85(3):845–881.
34. Aiello JS, Masters S. Fuchs's spot in the macula: a rare lesion seen in myopic patients. *Am J Ophthalmol*. 1953;36(8):1126–1128.
35. Yokoi T, Ohno-Matsui K. Diagnosis and treatment of myopic maculopathy. *Asia Pac J Ophthalmol (Phila)*. 2018;7(6):415–421.
36. Pi S, Hormel TT, Wei X, et al. Retinal capillary oximetry with visible light optical coherence tomography. *Proc Natl Acad Sci U S A*. 2020;117(21):11658–11666.